

THERMAL EXPANSION IMPACT ON VIBRO-DYNAMIC PROPERTIES OF BULB HYDROGENERATORS

Ozren Orešković
Veski d.o.o.
ozren.oreskovic@veski.hr

Ozren Husnjak
Veski d.o.o.
ozren.husnjak@veski.hr

Nicolas Dehlinger
Iris Power (Qualitrol)
ndehlinger@qualitrolcorp.com

Miljenko Brezovec
HEP Proizvodnja, PP HE Sjever
miljenko.brezovec@hep.hr

John Letal
Iris Power (Qualitrol)
jletal@qualitrolcorp.com

SUMMARY

Vibrodynamical behavior of bulb units, due to specific design and operating conditions, depend very much on the relative position of the rotor and stator as well as the bearings. Due to the horizontal shaft layout and the fact that the unit is submerged, rotor sag and construction thermal conditions have a large impact on the machine dynamic condition.

On two bulb units at the same plant, the condition was monitored for several years, with the purpose of investigating the correlation of excessive events (instabilities) to operating and start-up conditions. The monitoring system included rotor vibrations, air gap and flux, rotor pole temperatures, stator winding temperatures, axial displacements and process operating quantities (e.g. active and reactive power) as well as electrical values.

Especially prominent were the problems on unit B where cracks on the rotor rim appeared that could have been related to vibrations in combination with manufacturing defects. The monitoring system's comprehensive database enabled cross correlation of different values to assist in identifying the root cause of this instability, which appeared to happen quite unexpectedly. Detailed analysis of the data recorded by the monitoring system showed that the described vibrational instabilities were the result of the rotor thermal deformations and rotor's thermal imbalance likely related to the attachment between the rotor poles and the rotor rim.

Key words: Vibrations, generator, bulb unit, monitoring, deformations, imbalance

1. INTRODUCTION

Bulb hydrogenerating units get their name from the streamlined watertight housing style of turbine generator sets placed in a waterway structure. Bulb units are completely submerged in the water passage with the generator mounted horizontally within the bulb. The turbine is a propeller design with Kaplan style control of the blade position. Bulb units are typically in locations with continuous high flows but very low heads, in run-of-the-river schemes. Bulb hydrogenerating groups are generally low-speed (70-130 rpm), and low- to medium-output (below 100 MW). In North America, bulb units are installed along some of the major rivers, such as the Columbia, the Ohio or the Arkansas rivers. For example, 8 bulb units of 54 MW, 85 rpm are installed at the Rock Island powerplant along the Columbia river [6]. As of 2019, the largest bulb generating groups are installed in Brazil, at the Jirau hydroelectric powerplant [7]. While capable of harnessing the power of river with high flows and very low head better than other turbine designs can, one major inconvenience of a bulb hydrogenerating group comes from the fact that it is completely submerged. Consequently, maintenance on such units can be challenging. During inspection of bulb units, tests or repairs, and maintenance everything must go through the unit's access hatch. It is for this reason,

instrumenting bulb units with sensors and acquisition instruments for online monitoring and condition-based maintenance is beneficial.

The case study presented in this paper is about two similar hydroelectric turbine-generators (rated power 39 MW) with bulb turbines (runner diameter 5.5 m, speed 125 rpm, rated flow 250 m³/s, head 16-20m) that both experience dynamic instability during start up. The generator rotor consists of the shaft and rim. The rim is forged out of steel (not laminated) and has 48 poles. Because of limited space, the rotor pole coils are overlapped, common in bulb units. Poles are attached to the rim with 11 bolts along the axis. There are two guide bearings (generator and turbine) and one thrust in between the turbine and generator.

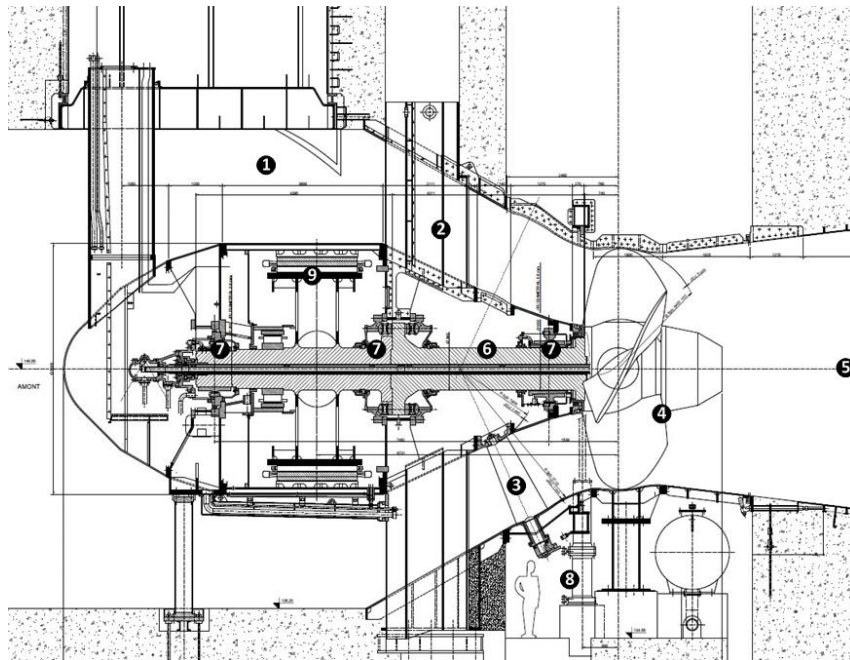


Figure 1 – Turbine-generator cross-section

The bulb generators design is shown in Figure 1 and the measurement sensor layout is shown in Figure 2. Probes are installed permanently, as a part of the on-line monitoring system and all the results are obtained using the same sensor configuration.

Instability is manifested through inconsistent vibration amplitudes during machine start up, happening on both units, more severe on unit B. On several occasions, vibration amplitudes were extremely high on Unit B. During one such event the relative shaft vibrations (S1n - Amplitudes) were measured up to 700 μm on the axial bearing (bearing with no radial clearance) and 250 μm (peak) on the generator guide bearing. For the reference, ISO 20816-5 recommendation for shaft displacement on guide bearings refer to 70% of bearing clearance (in cold state) as a tolerable limit for shaft displacement. For this generator a generator guide bearing clearance is 295 μm (on each side), meaning that in this case shaft displacements were as large as 85% of bearing clearance.

These extreme vibration amplitudes can cause a lot of stress on the shaft and rotor construction and possibly result in mechanical damage. During a regular overhaul after this event cracks were found on the shaft-to-rotor spider joints which could be related to this high vibration. The root cause of the instability has not yet been identified and similar events at lower amplitudes have occurred since the overhaul which did not lead to new cracks developing. This led to the additional analysis presented in this paper including several start up and coast down events.

The most promising conclusion is that excessive vibrations that appear to happen with no apparent or repeatable cause, are seemingly a result of the thermal processes and dilatations/contractions of the rotor construction during run down and start up events. The paper analyzes this mechanism of thermal dilatations and unbalance and shows that the thermal processes are not identical during every machine run down, standstill and run up. Therefore, the machine starting dynamic conditions are not identical and excessive vibrations can result from the residual strains accumulated from run down until the next start up. The paper also proposes the possible causes of the residual strain on the rotor.

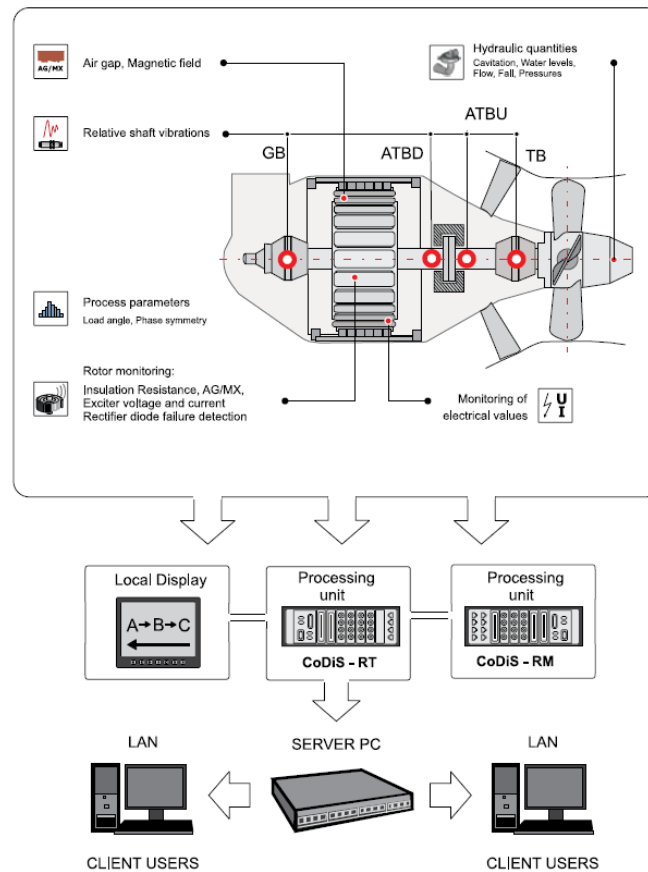


Figure 2 – Machine and sensor layout

2. EXCESSIVE VIBRATIONS EVENT DESCRIPTION

The first recorded event with high vibrations on Unit B was detected in May 2005 during the first run after a rotor replacement scheduled after 30 years in operation. The trend data of the shaft displacement amplitude at the machine rotating frequency, S_{1n} (first harmonic) are shown for vertical probes on turbine bearing, axial bearing downstream, axial bearing upstream and generator bearing in Figure 3. The system also has radial vibrations measured on the axial bearing, both radial bearings, and inside the air gap using the air gap probes and data analysis that enables accurate S_{1n} Amplitude and Phase calculation removed from air gap signal. This enables the plot of the dynamic shaft centerline from the turbine to the generator. This generator has a 6mm air gap, which is relatively small for a hydrogenerator. Therefore, the generator is very sensitive to magnetic unbalance. This first recorded event shows the following:

- Start, speed no-load
- Field flash ¹– cold
- Heating with field turned on
- Short field turned off
- Field flash and heating
- Field off – machine heated

The heating process influenced the vibration response and in combination with the magnetic field the vibration amplitudes increased. In addition, at speed no-load after the heating process, the vibration amplitudes were much higher comparing than when the machine was in the cold condition, 150 μm peak compared to 60 μm peak on the axial bearing. The amplitudes reduced as the machine cooled down spinning at speed no-load. The conclusion was that thermal bowing (thermal rotor line deformation) was

¹ Field flashing is used on self-excited generators, where the residual magnetism is not high enough to build up the terminal voltage when starting. What is done is to connect an external DC source to the field winding to start the voltage build up; the flashing source is removed for normal operation

causing the unbalance, both mechanical and electrical. After re-aligning the machine and additional balancing the machine was commissioned successfully.

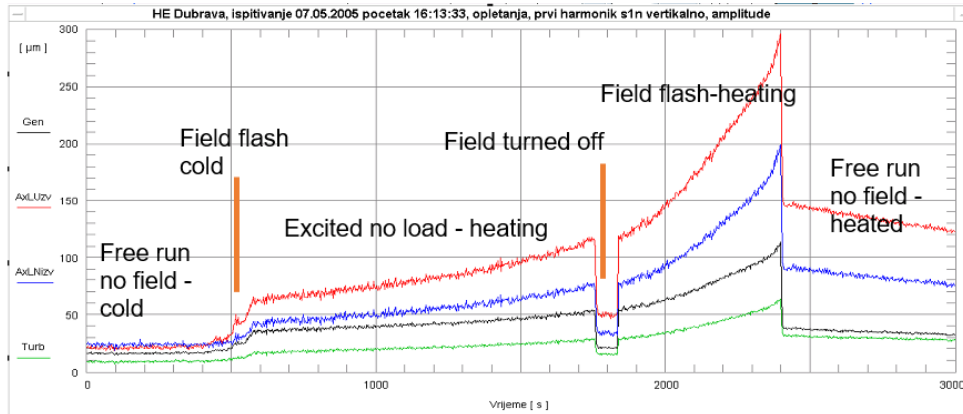


Figure 3 – vibration amplitudes in vertical direction on first harmonic, S1n in vertical direction (dir 2), recorded in first run after rotor replacement on Unit B in May 2005 / Red= Thrust bearing upstream; Blue= Thrust bearing downstream, Black= Generator, Green= Turbine

Figure 4 shows a similar such event recorded by the monitoring system after a regular start up in December 2011. The graph shows S1n amplitudes on all bearings. Shaft displacement on the Axial bearing (no radial clearance) increased up to 720 µm peak. The machine operating conditions were constant (both active and reactive power) during whole period. During an overhaul in January 2012 cracks were found in the shaft-to-rotor rim, likely related to this event, leading to longer downtime during this overhaul. Overhaul on bulb units include dewatering and taking the rotor out is quite complicated, so overhauls take long and are quite expensive.

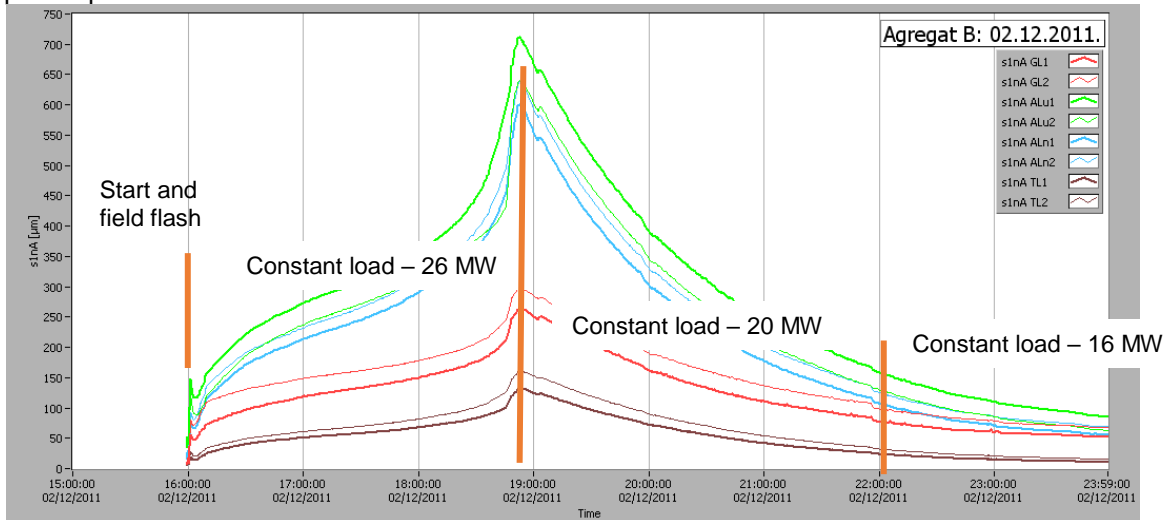


Figure 4 First harmonic of shaft displacement during Unit B machine operation in December 2011

Legend: S1nA = First harmonic Amplitude; GL1(2) Generator bearing direction 1(2); ALu1(2)= Thrust bearing upstream direction 1(2); ALn1(2)= Thrust bearing downstream direction 1(2), TL1(2)= Turbine bearing direction 1(2)

The cracks were fixed, rotor centered, and the machine was put back in operation with no root cause identified. After this event, a similar instability was detected by the monitoring system shown in Figure 5 with lower displacement amplitudes than in Figure 4. The shaft displacement on the Axial bearing upstream and downstream (ALU and ALN) started to rise while the machine was operating in steady state conditions. The vibration amplitude increase was constant even when the load was reduced, and the stator temperatures started to decrease. The rate of change was not linear and lowering the load had no effect on the amplitude rise. After this event, during steady state operation the vibration amplitudes reduced to normal condition at 50 µm peak. The first diagram in Figure 5 shows the axial bearing shaft displacement, the second shows the Active power and stator winding temperatures, the third diagram shows the S1n amplitudes of the rotor displacement inside the air gap, obtained from the air gap probes around the stator

circumference at 90°. The rotor displacements corresponded well with the axial bearing displacements. Any thermal bowing should be visible in the air gap data with consistent results at different poles.

The fourth diagram shows the minimum air gap trend on pole 1 and the fifth on pole 24. The monitoring system records the pole profile data for each probe which will have 48 minimums for each data set since there are 48 salient poles in this machine. The trends in diagrams 4 and 5 represent the air gap value for each probe at pole 1 and 24 because they display opposite results. For this event, the deflection was largest in direction from pole 1 to 24 since the minimum air gap value was smallest at pole 24 at the same time it was the largest at pole 1 indicating the rotor was closer to pole 24 during this event. It should be noted that for some of the other events the thermal bowing was in different directions. This data indicates that the shaft was bowing during these events, but the cause of the bowing is still unknown.

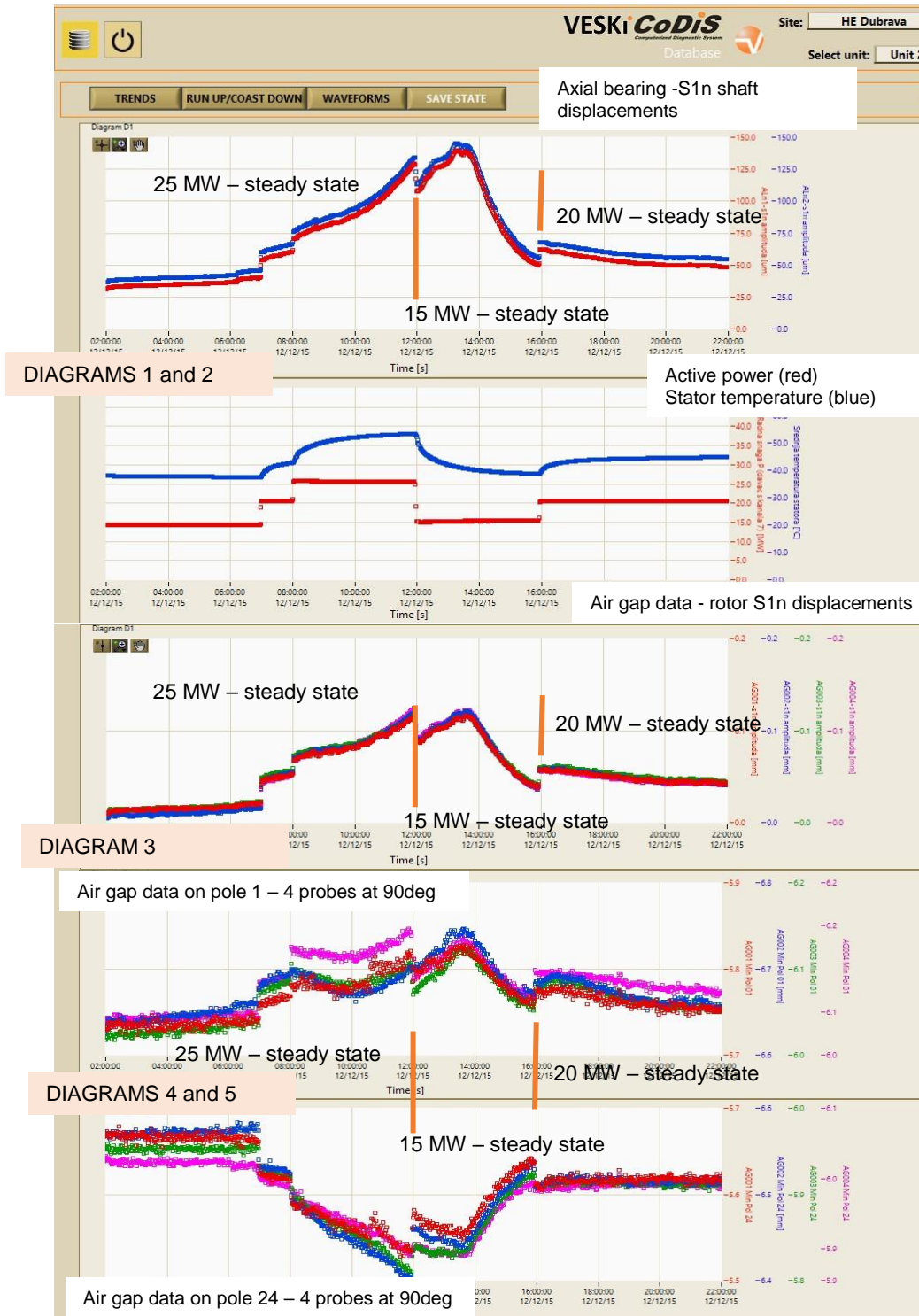


Figure 5 – trend diagrams for several cross-correlated values on Unit B

3. VIBRATION ANALYSIS DURING MACHINE START UP

Data during a start-up were used to get more insight and better define a root cause of the described behavior. The monitoring system records data continuously, even when machine is stopped. One of the signals measured and analyzed for vibration data is S_{max}^2 . S_{max} is recorded with and without a trigger (phase reference) so it is calculated even when machine is in slow roll and there is not enough data for harmonic analysis. Other values calculated from the same sensors, where no trigger is present are Peak-to-peak and static shaft centerline. They are also recorded during machine stop condition and were essential alongside air gap data to determine the root cause of this behavior.

Figure 6 shows the trend data for S_{max} on the Axial bearing upstream (ALU – red curve) and downstream (ALN-blue curve), Active power (green curve) and shaft Speed (Magenta curve) during two start up events on 10.01 and 11.01. 2016. The upper diagram represents the start-up on 11.01. The machine was turning in slow roll for 15 min before it went up to full speed and was connected to the power system and loaded. During slow roll, the monitoring system recorded high amplitude S_{max} on the axial bearing at approximately 120 μm that increased to 270 μm when the machine started to speed up. During the start-up on 10.01 shown on the lower diagram, the S_{max} during slow roll was much lower in comparison and there were no significant vibration amplitudes present when the machine sped up. This indicates that when thermal bowing is present during slow roll, the field flashing causes magnetic unbalance resulting in high vibrations during start-up. If the thermal bow is not present, then the vibration amplitudes remain low while the machine is speeding up.

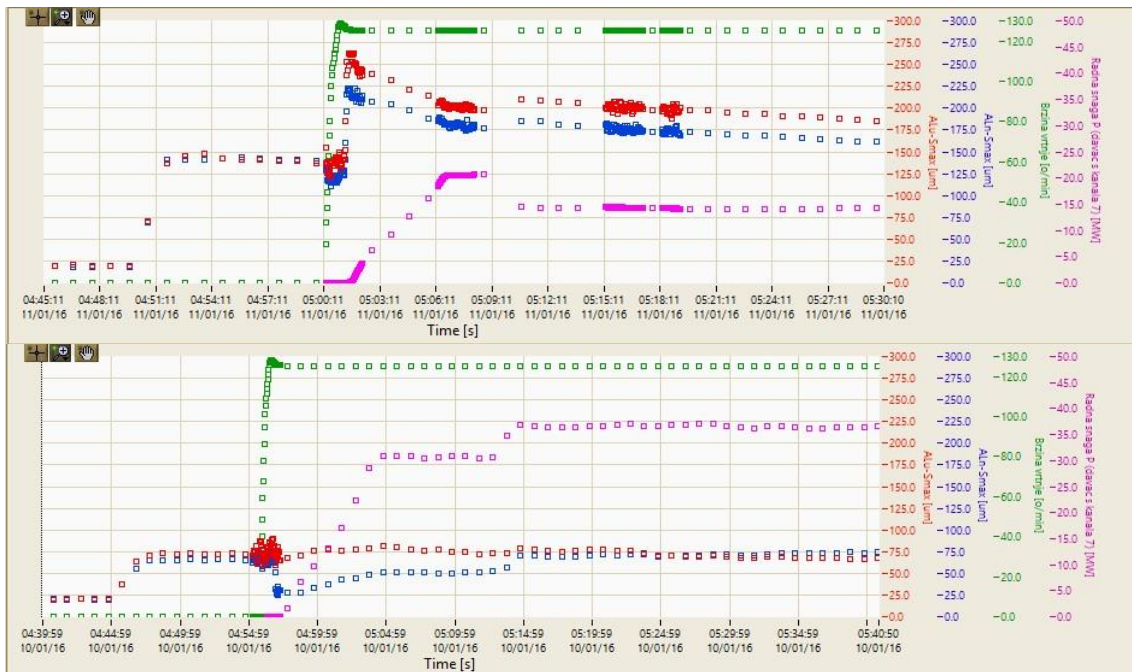


Figure 6 – Vibration response during two start up events recorded automatically by monitoring system

The slow roll shaft displacement was detected several times by the monitoring system automatically when the shaft vibration amplitudes triggered an alarm while the machine was speeding up. During alarm events the software captured raw data from all the probes for 36 seconds for post processing. One such event is shown in Figure 7, which represents the raw data from horizontal probes on all four bearings (TL – turbine / magenta curve, ALU – axial bearing upstream / blue curve, ALN – axial bearing downstream / green curve, GL – generator bearing / red curve). On the lower diagram is a shaft trigger – showing 1 turn in 14 sec ~4RPM. Even though machine had no dynamic forces present for such a low speed, it is visible that shaft displacements were relatively high. This indicates the shaft Run Out measured at slow roll was caused by thermal bowing. This bowing was not always the same since shaft geometry irregularities such as centerline Run Out would not always be present.

² S_{max} is the maximum displacement value obtained from two perpendicular probes as: $S_{max} = \sqrt{X^2 + Y^2}_{max}$

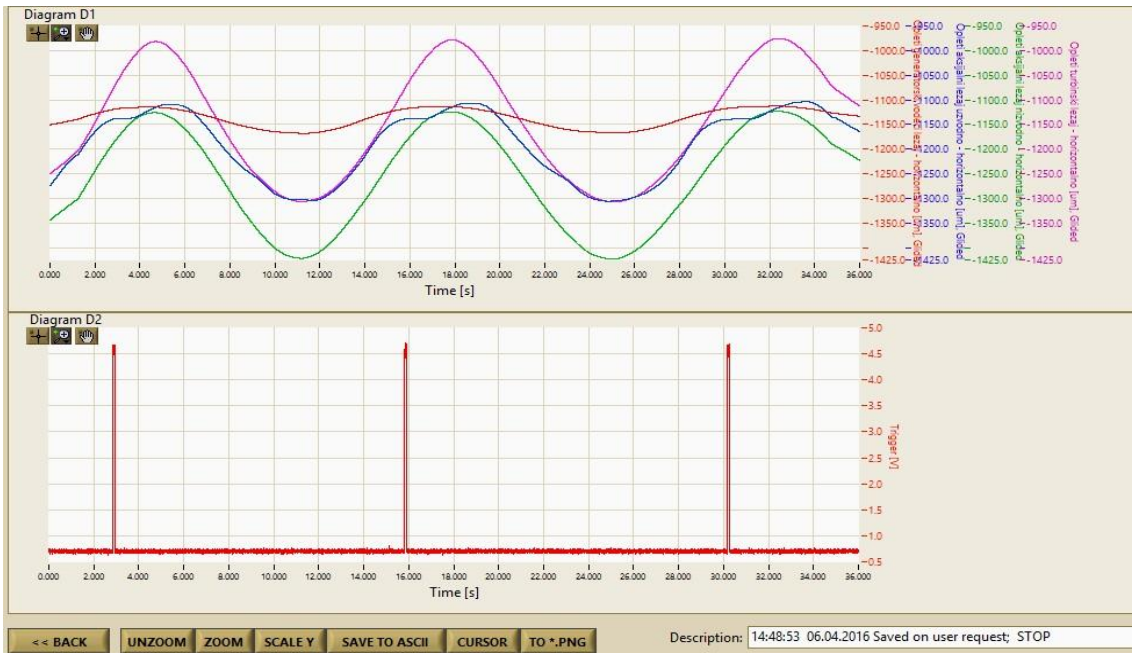


Figure 7 – Raw data recorded during slow roll, before machine start up.

To support this, air gap vibrations were observed during the same slow roll event as shown in Figure 8. The monitoring system treated this as a STOP condition, since the machine was turning at only 4 RPM. The polar rotor shape consists of the rotor pole distribution inside the air gap, recorded by each probe, with the rotor dynamic eccentricity extracted. The dynamic eccentricity is shown as the rotor center orbit on the first harmonic of rotational frequency, S_{1n} , on the same plot as a center of the rotor. The rotor dynamic eccentricity maximum displacement, S_{max} was 117 μm . That number was calculated from two perpendicular air gap probes in the same manner as the orbit and S_{max} were calculated from proximity probes. The peak-to-peak movement measured from the air gap would be equivalent to 190 μm , while machine was turning at only 4 RPM, and no significant dynamic forces were applied to it. This is consistent with the data measured by proximity probes and in line with the bowing shaft theory.

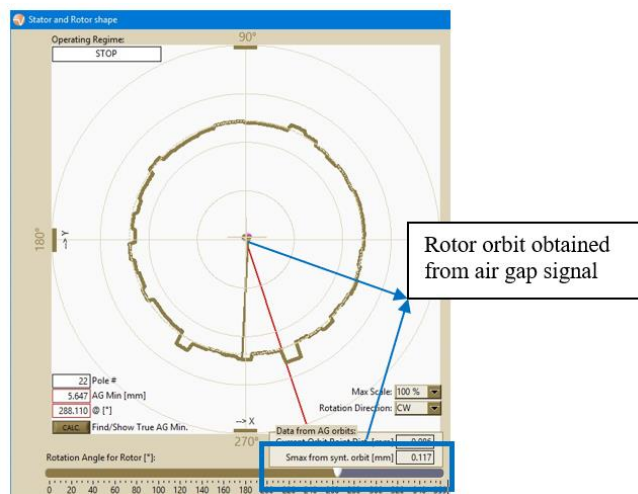


Figure 8 - Air gap polar plot at 4RPM consisting of air gap rotor pole/rim geometry and eccentricity

To further support that the cause of high vibrations during field flash was related to the shaft bowing, a comparison between the data before and after field flash was conducted during one run up and synchronization event recorded by the monitoring system, shown in Figure 9. The upper diagram represents the raw data of the Magnetic Field and the trigger signal. The lower two diagrams represent two events in time with a clear indication of the Magnetic Field impact on generator vibrations. The orbit plot inside the air gap indicates dynamic instability caused by the magnetic field, because the rotor bowing was present before the field flash event.

This is also visible as an orbit inside the air gap. In the cases where there was no bowing present on this machine, there was no sudden increase in vibrations with field flash.

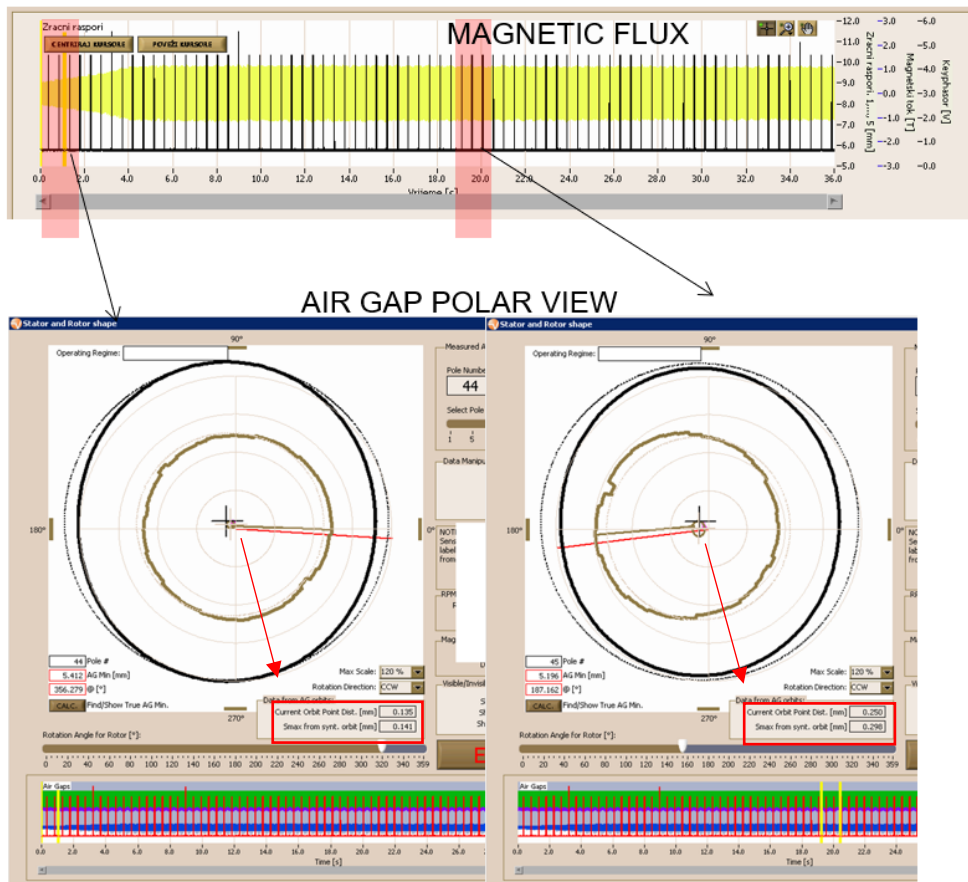


Figure 9 – Comparison between field flash and minimum field during start up and synchronization event

4. THERMAL DILATATIONS IMPACT ON VIBRATION RESPONSE

In order to determine the root cause of the high vibrations due to thermal bowing multiple starts and stops were observed in an attempt to find a pattern. The upper diagram of Figure 10 shows shaft displacement, S1n on Axial bearing in vertical direction, both upstream on ALU (red curve) and downstream on ALN (blue curve) of Unit A. Both units show similar behavior, Unit A was chosen because of the clear distinction between standstill and running events which helps in understanding the mechanism of the described problem. The lower diagram shows machine speed (red curve), shaft static centerline, vertical direction on ALU (blue curve) and horizontal direction on ALU (green curve).

The value of blue and green curves represents the physical distance from the shaft displacement probe to the shaft. So as the shaft was moving towards the probe the distance was approaching 0. S1n amplitudes were recorded only when the trigger (phase) was present, or when the machine was spinning. During some start-up events the vibrations were high and during others they were within normal values.

Static shaft centerline (DC) position was recorded when the machine was stopped which proved to be essential for root cause analysis of thermal bowing.

The largest changes of shaft static position was in the vertical direction during 48 hrs of stand still where the vertical shaft center position changed by 0.9 mm (900 μm) compared to only 0.25 mm (250 μm – not shown on this diagram) in the horizontal direction. The vertical sensor was above the shaft so the signal decreased as the rotor shaft lifted. This shows that during machine heating and cooling process there was significant change in the rotor line sagging in the vertical direction.

Figure 10 also shows the correlation between the shaft DC position signal and the high vibrations. The orange dashed line represents the threshold where this shaft DC signal had not reached the final levels, and the machine was experiencing high vibrations. The green dashed line represents those conditions where the shaft DC reached final levels and the machine did not experience high vibrations.

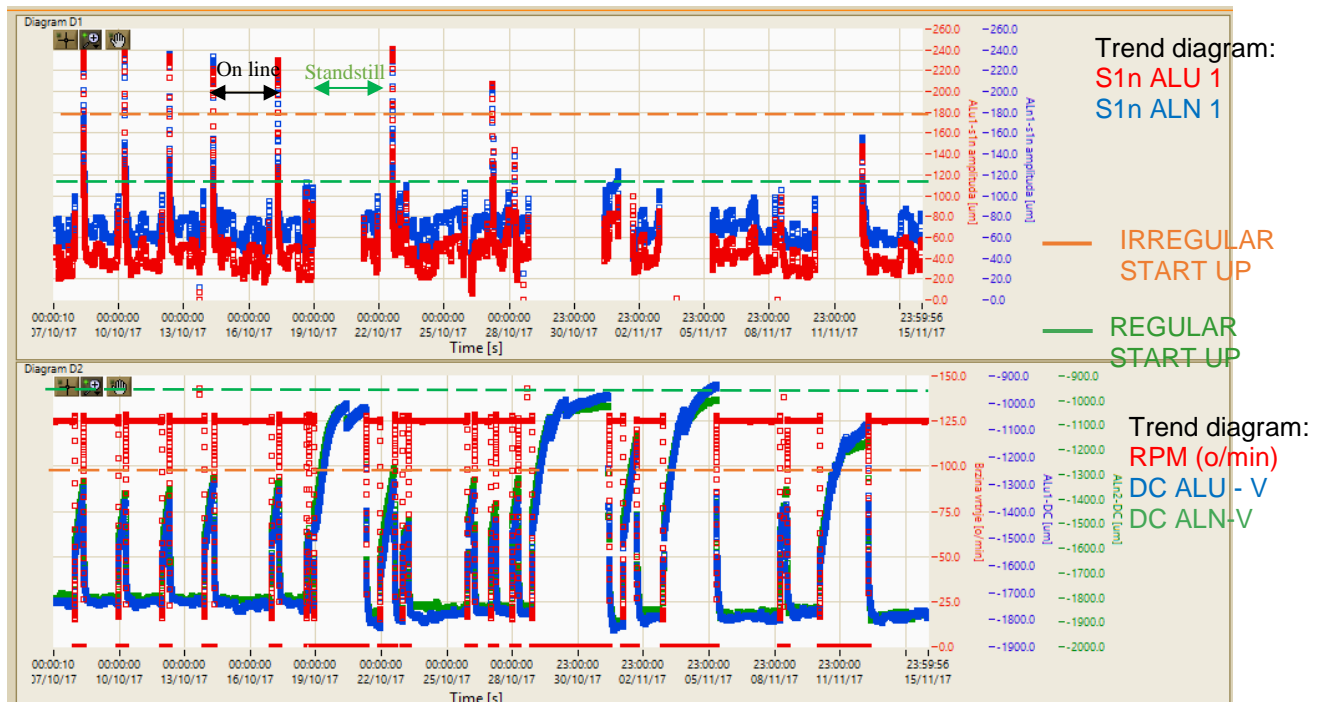


Figure 10 – Trend diagrams of multiple start and stop conditions on Unit A

The Shaft DC signal (lower diagram of Figure 10) shows sudden amplitude fluctuation during this process. It seems that suddenly a force was applied on the shaft center and it repositioned itself. However, the cooling process continued and so did the shaft centerline movement upward to the sensor as the thermal bow straightened. It is clearly visible in Figure 11 during one of the longer standstill conditions from Figure 10.

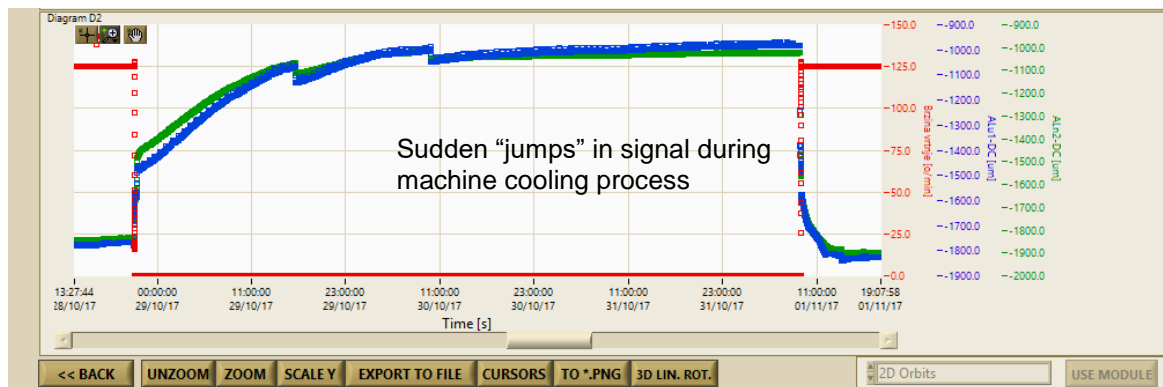


Figure 11 – Shaft DC position during stand still condition, on ALN – vertical direction

This indicates a resistance to reverse thermal dilatations during the cooling process as if something on the rotor resisted the shrinking process as the temperature decreased. During the “regular” startup condition 19/10/17) the static shaft DC amplitude showed that the shaft was approximately 250 μm closer to the probe when compared to the previous start-up. Comparing the vibration amplitudes to S1n amplitude difference on ALU1 (red curve), between that two starts show a similar measured value (difference in S1n is approximately 200 μm). The conclusion is that the residual rotor line sagging was present as a thermal bow during those irregular startups. Similar behavior was present during other events.

During longer cooling periods, approximately 30-48 hrs, the rotor line sagging was straightened with no bowing present. Therefore, vibrations were at normal amplitudes during those startups, as the machine was balanced for cold condition, or conditions relatively close to that. In other cases, the thermal bowing was still present which caused the problems described in this paper.

As of writing this, the root cause mechanism of this bowing has not yet been completely identified, but the described behavior indicates residual forces in the rotor are present during the machine cooling process while at standstill. The most probable cause is in the attachment of rotor pole to the rotor rim.

During operation at load, the rotor pole temperature was approximately 35-40°C higher than the rotor rim. Therefore, uneven rotor rim to pole heating and cooling could be one of the reasons for the bending forces to appear. This phenomenon is present on both units. The upper diagram in Figure 12 is for unit A and lower for Unit B of the same signals, Shaft DC position on ALU in the vertical direction (blue curve), shaft speed (red curve), and average stator temperature (green curve). Both time periods were selected when the starting point was taken after several days of standstill, during which the machine had a chance to completely cool down and stop re-positioning. Both machines had similar environmental conditions and cooling time should be similar to both machines for the selected time periods.

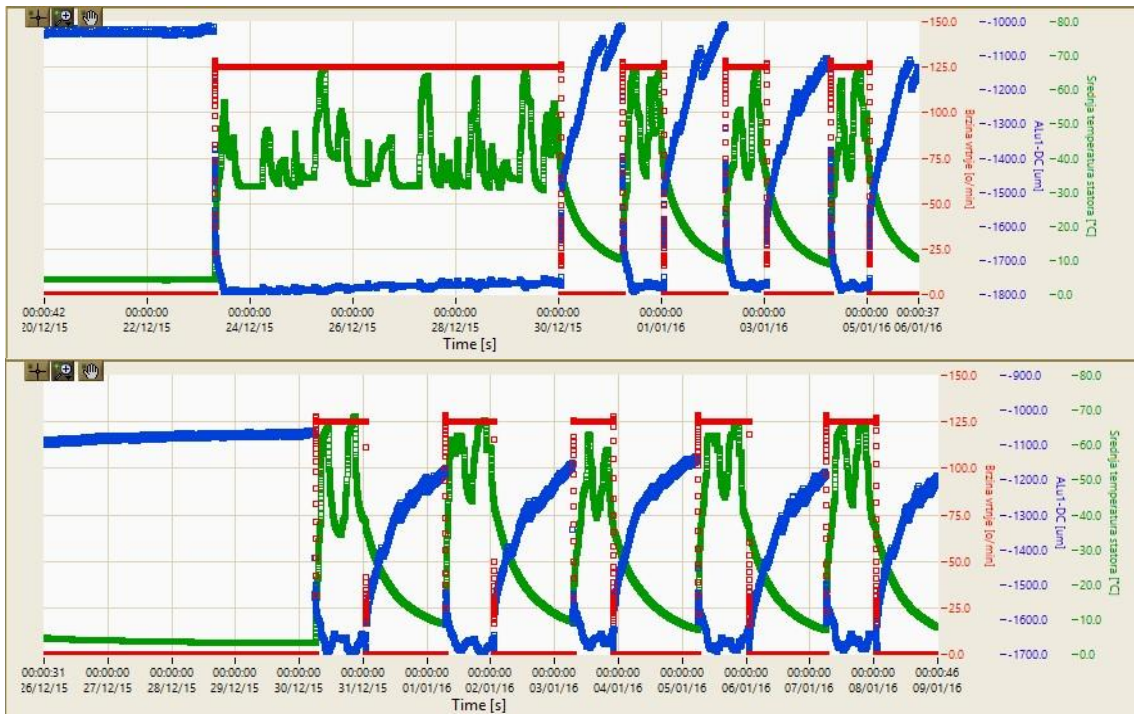


Figure 12 – Shaft DC position on Axial bearing and machine speed on Unit A (upper digaram) and Unit B (lower diagram) in same time period

The Shaft DC values can be used as a reference for comparison on each graph in Figure 12. Unit A shaft position reached a similar value in two stops, however not every time. Also, vibrations during those start-ups were low in amplitude, similar to the behavior shown on Figure 10. Unit B did not reach the same starting position even though the standstill lasted for 24 hours or more. As mentioned, both machines had the same environmental conditions (same time period, same water and air temperature) but they did not behave in similar manner. It can be concluded that the reason for this behavior lays in the different resistance to thermal deformations on both units. That resistance may be much higher on unit B, hence the larger amplitudes that resulted with the two mentioned events.

The cause of these deformations is still unknown. Considering the diagrams displayed and the machine design the conclusion is that the problem comes from the pole to rim attachment. The rotor rim cross section is shown on Figure 13. The poles on these machines are attached to the rim using 11 bolts. This type of attachment requires extreme caution during the tightening to ensure that poles are allowed to stretch and shrink adequately when heating and cooling.

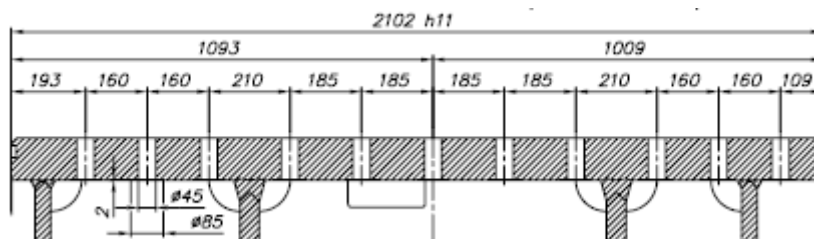


Figure 13 -Rotor rim cross section

If all the poles do not stretch or shrink equally, due to friction or inadequate tightening, an uneven force distribution may occur around rotor circumference, resulting in the rotor shaft to bow. This conclusion must be verified, but the data and conclusions in this paper can be used by OEM as a baseline for further investigation and eliminating the root cause.

5. CONCLUSION

Vibration and dynamic properties of bulb generators very much depend on thermal conditions. These conditions vary during operation as well as in standstill conditions. This paper concentrated on finding the root cause of sudden and unexpected high vibrations during start-up and sometimes even during steady state operation. Since such events could lead to cracks in the rotor body structure it is essential to determine the root cause and attempt to avoid such events in the future.

The results shown in this paper indicate residual thermal stress and deformations/bowing of the rotor line during standstill. This leads to increased vibrations during startup because of bowing and magnetic field forces which can, in some cases lead to severe vibrations and consequently cracks in machine parts.

The root cause is likely the pole to rim attachment, due to the specific machine design. Uneven pole contractions during machine cooling process leads to residual forces and rotor line bowing. If the machine cools down long enough or if it stops in the right position, the bowing is not present, but in most cases, due to operating conditions the bowing occurs, and the machine starts with higher vibrations.

LITERATURE

- [1] A. Muszynska: Rotordynamics, Taylor & Francis, 2005
- [2] C. M. Harris, A. G. Piersol: Harris shock and vibration handbook, McGraw Hill, 2002
- [3] M.Jadrić, B.Rajković, B.Terzić, V.Firinger, M.Despalatović, Ž.Gladina, G.Orešković, B.Meško, J.Macan: NADZOR HIDROAGREGATA - Stanje i razvoj u Hrvatskoj elektroprivredi, Proizvodno područje HE Jug, FESB 2004.
- [4] C. Major, G. Allen, Y. Houle: Benefits of ON-line Monitoring System in Operating and Refurbishing Generators at Rapide-des-Iles-Powerplant, UPDATING AND REFURBISHING HYDRO PLANTS VI, Montreal, October 1997
- [5] G.Orešković, O.Husnjak: "HE DUBRAVA, analiza vibracija agregata B 06.04 2012", TI 31042012 svibanj 2012.
- [6] Tidal Power, A. C. Baker, IET Digital Library, 1991, ISBN: 9780863411892
- [7] Jirau Hydroelectric Power Plant, Rondônia, digital paper from Power-Technology, available in May 2019 at: <https://www.power-technology.com/projects/jirau-hydroelectric-power-plant-rondonia/>